

Theoretical study on Surface-enhanced Raman scattering effects of gold nanoparticles in Terahertz range

ZHANG YONG-MING^a, REN GUANG-JUN^{a*}, BAI YU-KUN^b, YAO JIAN-QUAN^c

^a*School of Electronics Information Engineering; Tianjin Key Lab. Of Film Electronic & Communication Devices; Engineering Research Center of Communication Devices and Technology, Ministry of Education; Tianjin University of Technology; Tianjin 300384, PR China*

^b*School of Computer & Communication Engineering, Engineering Research Center of Communication Devices and Technology, Ministry of Education, Tianjin University of Technology; Tianjin 300384, PR China*

^c*College of Precision Instrument and Opto-electronics Engineering, Institute of Laser and Opto-electronics; Key Laboratory of Optoelectric Information Science and Technology, Ministry of Education, Tianjin University, Tianjin 300072, PR China*

We present here a theoretical analysis of the possibility to combine SERS with THz by investigating the electromagnetic enhancement effect of gold nanoparticles with visible to near-infrared and THz excitation. By means of the FDTD simulations, the electrical field enhancement, and thus the SERS enhancement factor of the gold nanoparticles with different sizes and interparticle separations are demonstrated, which indicate that the SERS effect exists in THz range as well and the SERS enhancement factor could reach 10^5 for 10 THz under the condition of certain size and interparticle distance. Therefore the SERS effect could be extended from ultraviolet, visible and near-infrared to THz regime.

(Received July 16, 2014; accepted June 09, 2016)

Keyword: Gold nanoparticles, SERS, Terahertz

1. Introduction

In the Raman scattering process, incident light is inelastically scattered from a sample and shifted in frequency by the energy of its characteristic molecular vibrations. The main advantage of Raman spectroscopy is its capability to provide rich information about the molecular structure of the sample, and thus it's widely used in biometrics and sensing technology. However, the Raman process has its intrinsic disadvantage owing to the very small cross section, typically 10^{-30} to 10^{-25} cm² per molecule, with the larger ones occurring only under certain resonance Raman conditions.^[1, 2] The discovery that there are enhancements of up to 5-14 orders of magnitude in the Raman signals being obtained for molecules adsorbed on rough surfaces of copper, silver, and gold, namely noble metallic nanostructures, which is known as surface-enhanced Raman scattering (SERS), solves this problem effectively and boosts the quite low detection sensitivity high enough in a new way and transforms Raman spectroscopy from a structural analytical tool to a structurally sensitive single-molecule and nanoscale probe.^[3-8] In recent years, SERS has attracted so plenty of interests for its remarkable enhancement that great contribution has been made to the development of fundamental and applied studies in fields as diverse as chemistry, physics, materials science, surface science,

nanoscience and the life sciences.^[3, 9-11] At present, the research on SERS is still on the way, and exploring the SERS based on broader electromagnetic spectrum should be considered.^[12-17] With numerous research data on SERS excited with ultraviolet, visible to near-infrared,^[18-20] a totally new field of SERS investigation is the excitation in the terahertz region for there are few reports being introduced from this angle.

Terahertz (THz, 1THz= 10^{12} Hz) wave, which lies in the frequency gap between the infrared and microwave, typically covers from 0.1 THz to 10 THz (wavelength 30 μ m-3mm). Since it could provide low-frequency (< 100cm⁻¹) absorption spectroscopy with information about intermolecular vibrations of some large molecules, such as chemical and organic molecules, THz spectroscopy is now widely used for low concentration sensing, analysis and imaging of biological tissue in natural applications and for sensitive detection of explosives, drugs, chemical and biological agents in security applications.^[21, 22] However, the power of the available THz sources is still rather low, thus limiting applications in which high intensities are needed^[21]. Therefore, the large field enhancement that SERS can offer may be critical for the development of novel application of THz radiation. Besides, in view of the fact that low-frequency Raman spectroscopy can also reflect vibration characteristics of the large molecules,^[1, 2] it's possible that combining low-frequency Raman

spectrum with THz excitation through SERS.

While the physical mechanism underlying SERS is still not fully understood now, it is widely accepted that the SERS can be discussed in terms of electromagnetic and chemical enhancements, in which the former term is responsible for the major portion of SERS enhancement up to 10^5 - 10^{12} while the latter is quite weak as 10-100 in most cases.^[6, 8, 23] Electromagnetic enhancement is mainly caused by the excitation of collective oscillations of the conduction electrons in a metal nanoparticle defined as surface plasmons.

The electromagnetic enhancement factor can be expressed as:^[24]

$$G^{SERS} = \left| \frac{\hat{E}_{loc}}{\hat{E}_0}(\omega_i) \right|^2 \left| \frac{\hat{E}_{loc}}{\hat{E}_0}(\omega_R) \right|^2 \quad (1)$$

where ω_i , ω_R is the angular frequency of incident light and the Raman light, respectively. \hat{E}_{loc} , \hat{E}_0 is the absolute value (the normalization of incident light and the Raman light) of the local electric field with and without metallic substrate, respectively. The enhancement factor results from the enhancement of the Raman radiation in a two-step-process: Firstly, the excitation of Raman-active molecules is in proportion to the square of the local electric field $\left| \frac{\hat{E}_{loc}}{\hat{E}_0}(\omega_i) \right|^2$ at the incident frequency which can be very high on metallic surface. In the second step, the emitted Raman radiation is enhanced by the metal particle resonance which is in proportion to the local electric field at the Raman light frequency $\left| \frac{\hat{E}_{loc}}{\hat{E}_0}(\omega_R) \right|^2$. In most cases, the frequency of the Raman scattering is close to that of the incident radiation so that the electromagnetic enhancement factor can be expressed as:

$$G^{SERS} = \left| \frac{\hat{E}_{loc}}{\hat{E}_0}(\omega_i) \right|^4 \quad (2)$$

namely, the enhancement factor is the fourth power of the E-field amplitude and thus it can cause a remarkable SERS effect even if the increase in the local electric field is usually modest.^[25]

What's more, much recent research has focused on the development of an understanding of how the structural properties of metallic nanostructures can be optimized to provide the largest possible electromagnetic field enhancements. These studies have shown that the largest enhancement factors typically occur in junctions between coupled nanoparticles when excited by light polarized across the junction between the particles.^[16, 26] The intense electric fields induced in such junctions when excited by light of a wavelength in resonance with the coupled nanoparticle plasmon are believed to be the "hot spots" for

Raman scattering which dominates the observed SERS signal in more complex nanoparticle aggregates. Such field enhancements can strongly enhance the Raman scattering if probe molecules are located in the junctions between the two nanoparticles.^[27, 28]

In addition, electromagnetic enhancement is irrelevant to the adsorbed molecules and is critically dependent not only on the nature of the metal but also on the size, shape and interparticle coupling of nanoparticles, and the frequency of the incident light.^[29, 30] Ever expanding techniques in nanoscience have provided great opportunities to fabricate a wide variety of nanostructures with controllable size and shape. Research on the optimal nanostructures is always of central concern to gain the highest SERS activity. Since gold is one of the most widely used substrate, extensive efforts have been made to optimize the SERS activity of gold nanoparticles with different sizes.^[26, 31, 32] Therefore, it's worthy of performing a systematic study on the SERS of Au nanoparticles, especially in THz region.

2. Simulation

In this work, we propose an application of the three dimensional FDTD (3D Finite-Difference Time-Domain) to SERS. The 3D-FDTD has proven to be well adapted for spectroscopic studies^[33, 34] and the results obtained from the numerical simulations and the corresponding experiments are in good agreement. The versatility and flexibility of the 3D-FDTD suggests its possible application to the study of the surface plasmons and the influence of different parameters such as the size and the shape of the nanoparticles on the position of the maximum of the SERS intensity.^[24]

The 3D-FDTD simulation was carried out with FDTD SOLUTIONS software (version 8.6.0) provided by Lumerical Solutions, Inc. The dielectric constants of gold in visible to near-infrared range were taken from the material database built-in, while that in THz band were derived from Drude-Lorentz dispersion model, which accurately describes the dispersion function of gold in the modeling of extinction spectra from visible frequencies to THz.

The Lorentz-Drude Model can be expressed as this equation:

$$\varepsilon_r(\omega) = \varepsilon_{r,\infty} + \sum_{m=0}^M \frac{G_m \Omega_m^2}{\omega_m^2 - \omega^2 + j\omega\Gamma_m} \quad (3)$$

Where $\varepsilon_{r,\infty}$ is the relative permittivity in the infinity frequency and $\varepsilon_{r,\infty} = 1$ here. Ω_m is the plasma frequency, ω_m is the resonant frequency, and Γ_m is the damping factor or collision frequency. Lorentz-Drude Model parameters of Au with angle frequency (rad/s) are as follows^[35]:

The dielectric constants are got through Equation 3 and shown in Fig. 1.

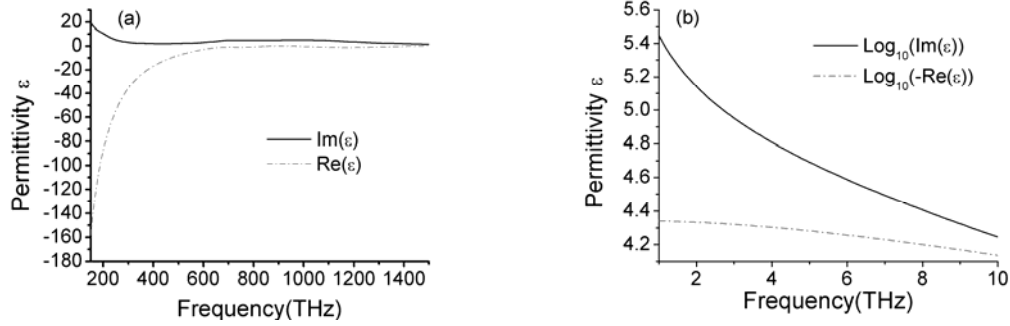


Fig. 1. Complex permittivity of gold at visible to near-infrared frequencies (a) and at THz frequencies (b) calculated using the Lorentz-Drude model. The red dashed lines correspond to the real component of the permittivity (absolute value in (b)), while the black lines correspond to the imaginary component.

Table 1. Parameters in Lorentz-Drude model for gold.

Term	Strength G_m	Plasma Frequency Ω_m	Resonant Frequency ω_m	Damping Frequency Γ_m
0	0.7600	0.137188×10^{17}	0.000000×10^{00}	0.805202×10^{14}
1	0.0240	0.137188×10^{17}	0.630488×10^{15}	0.366139×10^{15}
2	0.0100	0.137188×10^{17}	0.126098×10^{16}	0.524141×10^{15}
3	0.0710	0.137188×10^{17}	0.451065×10^{16}	0.132175×10^{16}
4	0.6010	0.137188×10^{17}	0.653885×10^{16}	0.378901×10^{16}
5	4.3840	0.137188×10^{17}	0.202364×10^{17}	0.336362×10^{16}

In the simulation, we used Total-field scattered-field as excitation source. On the basis of the previous experience, the local electric field enhancements vary with the direction of the incident polarization, i.e., the SERS intensity of the molecules adsorbed on the metallic nanoparticles exhibit a strong polarization dependence. It is shown that the field enhancements are largest for polarization parallel to the direction across the centers of nanoparticles but almost none for polarization perpendicular to that direction,^[36] and the largest enhanced field in the gaps between the coupled nanoparticles is the “hot spots” mentioned above. We chose the first one in all cases.

As shown in the Fig. 2, the incident direction is along y-axis while the polarization is along z-axis. Ten values of D (diameter) of nanoparticles are selected from 20 nm to 200 nm, whereas ten values of the gap distance d are taken from 1 nm to 10 nm. We also consider that nanoparticles are placed in vacuum and that there is no substrate.

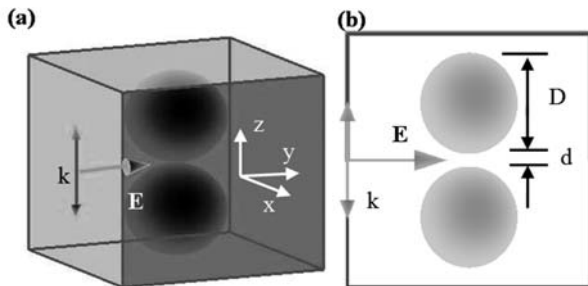


Fig. 2. Source and Structure definition for 3D-FDTD simulation. (a) In the 3D model, the incident light is along y-axis and the polarization is along z-axis. (b) The electric-field was evaluated in x-z plane. D is the diameter of the sphere and d is the gap distance.

The simulations of the electric-field distribution in the xz-plane at $y=0$, and the calculations of the field enhancement were performed in the middle of the gap of the gold particles junction.

3. Results and discussion

For the visible to near-infrared frequencies, Fig. 3 shows the relation between SERS enhancement factor G, particle size D and gap distance d under the 632.8 nm excitation. With a fixed d, the enhancement value keeps on increasing with increase in the particle size until about 120 nm. Then the overall trend tends to decline a little, thereby decreasing the field enhancement and accordingly resulting in a weaker SERS activity. And the smaller d, the greater G, which is resulted from interparticle coupling effects.^[37] As inset illustrates, with $D=120$ nm, G decreases gently when d is less than 4 nm and then obviously for the weaker interparticle coupling effects. Limited by the computing resource, the minimum d is set 1 nm to ensure accuracy. The calculation results show good agreement with the previous experiment data^[38] and thus demonstrates the effectiveness of 3D FDTD.

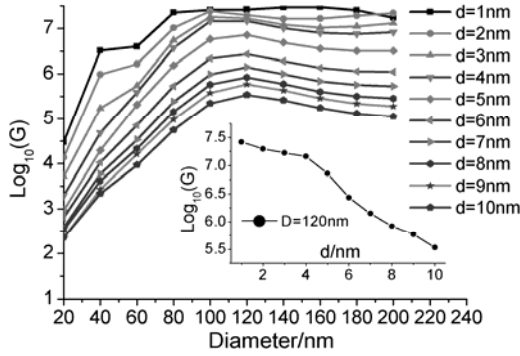


Fig. 3. Calculated SERS enhancement-factor G in the logarithmic scale for Au dimers system in the middle of the gap with the parallel polarization configuration as a function of the particles' size for different gap distances d , while the inset shows that G as a function of d for a 120 nm Au dimer. The excitation wavelength is $\lambda=632.8$ nm.

Based on the simulation result, we select an optimal dimer with $D=120$ nm and $d=1$ nm to find the wavelength in resonance with the coupled nanoparticle plasmon. In this case the wavelength considered is the one that gives rise to the maximum electric field. As shown in Fig. 4(a), the electric field is enhanced in visible range on a larger scale and the maximum corresponds to $f=400$ THz, namely $\lambda=750$ nm. Then the spatial distribution of the normalized electric field is got to Fig. 4(b). The huge enhanced field which is about 94 brings us the quite remarkable SERS enhancement factor G of up to 7.8×10^7 .

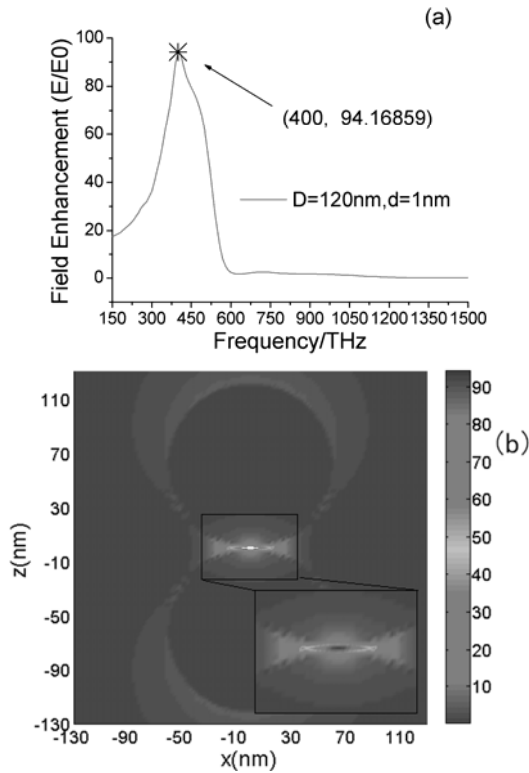


Fig. 4. (a) Field enhancement (E/E_0) evaluated in the middle of the gap of the gold junction as a function of the light wavelength in visible to near-infrared range in the case of particle size $D=120$ nm and gap distance $d=1$ nm. (b) Spatial distribution of the field intensity (normalized by the incident one) in the x - z plane for gap distance $d=1$ nm. The wavelength of the illuminating light is $\lambda=750$ nm.

For the THz frequencies, Fig. 5 presents the SERS enhancement factor G versus dimer size D for different junction spacing d illuminated with light of 10 THz. All the lines in the figure illustrate that G obtains a continual increase when D is enlarged, leading to the greatest G more than 5×10^5 occurs at $D=200$ nm. In all cases, $d=4$ nm corresponds to the largest G .

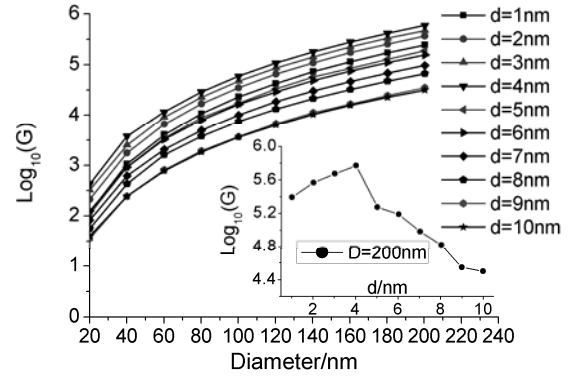


Fig. 5. Same as in Fig.3 but for the dimer size in the inset is 200 nm and the excitation frequency is $f=10$ THz.

Inset shows that the increase of G is broken seriously as d becomes larger than 4 nm with $D=200$ nm, and then G become smaller and smaller.

Therefore, we employed the dimer that $D=200$ nm and $d=4$ nm to find the suitable frequency making G largest. As shown in Fig. 6 (a), higher frequencies own higher field enhancements, then the spatial distribution of the normalized field intensity of 10THz is shown in Fig. 6 (b).

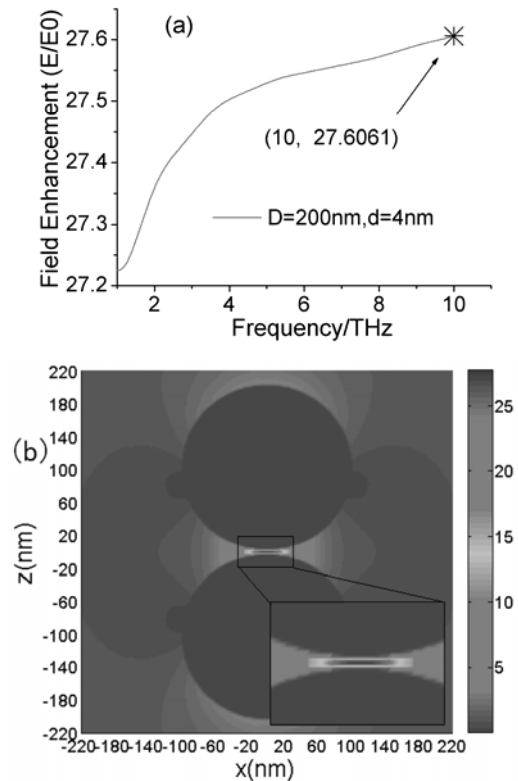


Fig. 6. Same as in Fig.4 but for the excitation frequencies are in THz range and particle size $D=200$ nm and gap distance $d=4$ nm for (a), and the excitation frequency in (b) is $f=10$ THz.

By contrast, the SERS enhancement factors of the visible are larger than that of the THz at certain size gold nanoparticle, for instance, $D=100\text{nm}$, all the G of the visible are above 5 while that at THz are under 5. Moreover, in Figure 6 (a), the difference between the field enhancements of each frequency in THz band is not that much and their values are a lot smaller compared with that of visible since the whole THz frequencies are beyond the strong surface plasmon polaritons condition due to the higher plasma frequency of metal.^[39, 40]

Still and all, SERS in the THz regime is considerable based on the simulation result that the SERS enhancement factor of THz increased by nearly 6 orders of magnitude, which is sufficient enough for practical applications. And the ever expanding techniques in nanoscience on fabricating a wide variety of nanostructures with controllable size and shape provides the foundation for the combination of SERS and THz since the SERS activity is better for larger particle size with appropriate gap separation in the THz range. Furthermore, as Katrin Kneipp supposed,^[8] we could go further to explore more material even envision synthetic if they contain a high density of free carriers. Taking into account of the fact that the permittivities of some semiconductor at THz frequencies and gold in the visible are similar,^[39, 40] we expect the application of SERS on these substrates in THz range.

4. Conclusions

In summary, we quantitatively simulated the local electromagnetic field enhancement around the illuminated Au nanoparticles with various sizes and interparticle distances in visible to near-infrared and THz range by FDTD, and proved the existence of the electromagnetic enhancement effect at THz frequencies, which extends SERS effect from ultraviolet, visible and near-infrared to THz regime. As a preliminary exploration of SERS with THz, this work is of considerable significance for further research.

Acknowledgements

This research was supported in part by the National Basic Research Program of China (Grant No. 9732010CB327801).

References

- [1] I.R. Lewis, H. Edwards, Handbook of Raman spectroscopy: from the research laboratory to the process line, CRC Press, Florida (2001).
- [2] B. Schrader, Infrared and Raman spectroscopy: methods and applications, John Wiley & Sons, Weinheim (2008).
- [3] A. Campion, P. Kambhampati, Chem. Soc. Rev. **27**, 241(1998).
- [4] P. Etchegoin, H. Liem, R. Maher, L. Cohen, R. Brown, H. Hartigan, M. Milton, J. Gallop, Chemical physics letters **366**, 115(2002).
- [5] H.G. Edwards, Analyst **129**, 870(2004).
- [6] C.L. Haynes, A.D. McFarland, R.P.V. Duyne, Analytical Chemistry **77**, 338 A(2005).
- [7] K. Kneipp, H. Kneipp, H.G. Bohr, Single-molecule SERS spectroscopy, Surface-Enhanced Raman Scattering, Springer, 2006, p. 261.
- [8] K. Kneipp, M. Moskovits, H. Kneipp, Physics Today **60**, 40(2007).
- [9] K. Kneipp, M. Moskovits, H. Kneipp, Surface-enhanced Raman scattering: physics and applications, Springer, (2006).
- [10] G. Braun, S.J. Lee, M. Dante, T.-Q. Nguyen, M. Moskovits, N. Reich, Journal of the American Chemical Society **129**, 6378(2007).
- [11] X. Lu, D.R. Samuelson, Y. Xu, H. Zhang, S. Wang, B.A. Rasco, J. Xu, M.E. Konkel, Analytical chemistry **85**, 2320(2013).
- [12] Z. P.X., G. W.L., L. X.Y, Spectroscopy and Spectral Analysis **7**, 1(1987).
- [13] A. Kudelski, Polish Journal of Chemistry **79**, 1551(2005).
- [14] Z.-Q. Tian, Journal of Raman Spectroscopy **36**, 466(2005).
- [15] M.K. Hossain, Y. Ozaki, Current Science (00113891) **97**, (2009).
- [16] D. Cialla, A. März, R. Böhme, F. Theil, K. Weber, M. Schmitt, J. Popp, Analytical and bioanalytical chemistry **403**, 27(2012).
- [17] B. Sharma, R.R. Frontiera, A.-I. Henry, E. Ringe, R.P. Van Duyne, Materials today **15**, 16(2012).
- [18] Z.-Q. Tian, Z.-L. Yang, B. Ren, D.-Y. Wu, SERS from transition metals and excited by ultraviolet light, Surface-Enhanced Raman Scattering, Springer, 2006, p. 125.
- [19] L. Cui, D.-Y. Wu, A. Wang, B. Ren, Z.-Q. Tian, The Journal of Physical Chemistry C **114**, 16588(2010).
- [20] Z. Yang, Q. Li, Y. Fang, M. Sun, Chemical Communications **47**, 9131(2011).
- [21] S.L. Dexheimer, Terahertz spectroscopy: principles and applications, CRC press, (2007).
- [22] Y. Shen, J Electr Electron Syst **3**, e113(2013).
- [23] C.L. Haynes, C.R. Yonzon, X. Zhang, R.P. Van Duyne, Journal of Raman Spectroscopy **36**, 471(2005).
- [24] N. Felidj, J. Aubard, G. Levi, J. Krenn, A. Hohenau, G. Schider, A. Leitner, F. Aussenegg, Applied Physics Letters **82**, 3095(2003).
- [25] H. Xu, Applied physics letters **85**, 5980(2004).
- [26] J. Mock, S. Norton, S.-Y. Chen, A. Lazarides, D. Smith, Plasmonics **6**, 113(2011).
- [27] H. Wang, C.S. Levin, N.J. Halas, Journal of the American Chemical Society **127**, 14992(2005).
- [28] P. Chu, D. Mills, Physical Review B **77**, 045416(2008).
- [29] L.J. Sherry, S.-H. Chang, G.C. Schatz, R.P. Van Duyne, B.J. Wiley, Y. Xia, Nano letters **5**, 2034(2005).

- [30] M.J. Natan, Faraday discussions **132**, 321(2006).
- [31] P.N. Njoki, I.-I.S. Lim, D. Mott, H.-Y. Park, B. Khan, S. Mishra, R. Sujakumar, J. Luo, C.-J. Zhong, The Journal of Physical Chemistry C **111**, 14664(2007).
- [32] A.R. Guerrero Hernandez, (2014).
- [33] K.S. Kunz, R.J. Luebbers, The finite difference time domain method for electromagnetics, CRC press, (1993).
- [34] S.C. Hagness, A. Taflove, (2000).
- [35] A.D. Rakic, A.B. Djurišić, J.M. Elazar, M.L. Majewski, Applied optics **37**, 5271(1998).
- [36] W. Hong, X. HongXing, SCIENCE CHINA Physics, Mechanics Astronomy **1**, 001(2010).
- [37] H. Xu, E.J. Bjerneld, J. Aizpurua, P. Apell, L. Gunnarsson, S. Petronis, B. Kasemo, C. Larsson, F. Hook, M. Kall, International Society for Optics and Photonics, p. 35, 2001.
- [38] W.-d. HUANG, B. REN, Spectroscopy and Spectral Analysis **29**, 1222(2009).
- [39] V. Giannini, A. Berrier, S.A. Maier, J.A. Sánchez-Gil, J.G. Rivas, Optics express **18**, 2797(2010).
- [40] J. Gómez Rivas, A. Berrier, Terahertz plasmonics with semiconductor surfaces and antennas, Microwave Conference, 2009. APMC 2009. Asia Pacific, IEEE, p. 1293, 2009.

*Corresponding author: rgj1@163.com
568220051@qq.com